



Soil parameter identification for cyclic loading

Aurélie Papon, Zhen-Yu Yin, Kevin Moreau, Yvon Riou, Pierre-Yves Hicher

► To cite this version:

Aurélie Papon, Zhen-Yu Yin, Kevin Moreau, Yvon Riou, Pierre-Yves Hicher. Soil parameter identification for cyclic loading. 7th European Conference on Numerical Methods in Geotechnical Engineering (NUMGE 2010), Jun 2010, Trondheim, Norway. pp.113–118. hal-01736235

HAL Id: hal-01736235

<https://hal.insa-toulouse.fr/hal-01736235>

Submitted on 20 Apr 2018

HAL is a multi-disciplinary open access archive for the deposit and dissemination of scientific research documents, whether they are published or not. The documents may come from teaching and research institutions in France or abroad, or from public or private research centers.

L'archive ouverte pluridisciplinaire **HAL**, est destinée au dépôt et à la diffusion de documents scientifiques de niveau recherche, publiés ou non, émanant des établissements d'enseignement et de recherche français ou étrangers, des laboratoires publics ou privés.

Soil parameter identification for cyclic loading

A. Papon, Z.-Y. Yin, K. Moreau, Y. Riou & P.-Y. Hicher

Research Institute in Civil and Mechanical Engineering, UMR CNRS 6183, Ecole Centrale de Nantes, France

ABSTRACT: An identification of soil parameters is performed by inverse analysis of two undrained triaxial cyclic tests on normally consolidated clay (kaolinite). A two-surface plasticity model is used for simulations and genetic algorithms are selected for the optimization procedure. First the problem of inverse analysis is formulated as a mono-objective problem, so that each test is considered separately and both sets of solutions are analyzed. Secondly, in order to take into account simultaneously the results of both tests, a multi-objective problem is considered and solved with a multi-objective genetic algorithm, which provides a set of equivalent solutions in terms of Pareto. Considering this set, a tradeoff is determined in order to fit at best the experimental and numerical curves for both tests and the relevance of the selected constitutive model is discussed.

1 INTRODUCTION

Fatigue in soils is a relevant phenomenon for many structures such as wind power plants, offshore installations, embankment, railway and tunnel (Andersen 2009). To obtain reliable results for the design of structures, the constitutive model has to be able to reproduce with good accuracy the cyclic behavior of soil. An accumulation of permanent strains during cyclic loadings with a possible stabilization depending on the applied stress level is often observed. For this purpose, models based on extension of the classical theory of elastoplasticity have been developed.

At the same time, the development of sophisticated constitutive models with increasing number of parameters leads to complex identification process for soil parameters. Satisfactory parameter identification from laboratory or in-situ tests is needed for engineering practice. Therefore, new techniques of resolution accounting for the characteristics of inverse analysis have been performed.

In this paper, a modification is made on the two-surface model of Al-Tabbaa (1987) to describe undrained cyclic behavior of clay with high number of cycles. A new method of soil parameter identification by inverse analysis is proposed. Then, these principles are applied to undrained triaxial cyclic tests on normally consolidated clay (kaolinite). Finally conclusions on the identification of the parameters and on the relevance of the model are drawn.

2 CONSTITUTIVE MODEL

2.1 Choice of the model

As aforementioned, the classical theory of elastoplasticity has been extended for a better representation of plastic strains during cyclic loading. Bounding surface plasticity for soil models, described by Dafalias & Hermann (1982), generates plastic strains within the bounding surface depending on the variation of the hardening modulus. This modulus varies from a high value when the stress point is far from the bounding surface, to a lower value when the stress point is on the bounding surface. Therefore, the model guarantees a smooth transition between elasticity and elasto-plasticity. However bounding surface plasticity assumes a purely elastic behavior, whereas experiments show a limited elastic domain, during unloading.

Kinematic hardening models consider kinematic yield surfaces within the bounding surface. Mroz (1967) propose a set of kinematic nesting surfaces with constant hardening moduli. As long as the stress point is within the smallest kinematic surface, the behavior is assumed to be elastic. As soon as the stress point reaches the smallest kinematic surface, the behavior becomes elasto-plastic with respect of the corresponding hardening modulus and the surface follows the stress path. If the stress point reaches the next nesting surface, the hardening modulus associated with it becomes relevant and both surfaces are dragged along the stress path. This strategy makes the storage of loading history possi-

ble and a stepwise decrease of the hardening modulus.

A two-surface model has been proposed by Al-Tabbaa (1987) and described by Muir Wood (1991) as an intermediate solution between a bounding surface model and a multi-surface model. This model provides a smooth decrease of the hardening modulus and a memory of the previous stress path. Because of its simplicity and its interesting properties, a model of this type is selected for this study.

2.2 Principles of the model

The two-surface model, developed by Al-Tabbaa (1987), is an extension of the modified Cam Clay model, where a kinematic yield surface is introduced within the bounding surface. The behavior is assumed to be elastic within the kinematic yield surface. The bounding surface corresponds to the modified Cam Clay yield surface:

$$F_b = \left(p' - \frac{p'_c}{2} \right)^2 + \frac{3(s:s)}{2M^2} - \frac{p'^2_c}{4} \quad (1)$$

where p' = mean effective stress; p'_c = value of the mean effective stress at the intersection of the current swelling line with the isotropic compression line; s = deviatoric stress tensor; and M = slope of the critical state line in q - p' space. The kinematic yield surface has the same shape as the bounding surface:

$$F_y = (p' - p'_a)^2 + \frac{3((s - s_a):(s - s_a))}{2M^2} - \frac{R^2 p'^2_c}{4} \quad (2)$$

where p'_a = mean effective stress at the center of the kinematic yield surface; s_a = deviatoric stress tensor at the center of the kinematic yield surface; and R = ratio between the sizes of the kinematic surface and of the bounding surface. The ratio R is assumed to be a model parameter.

The bounding surface evolves according the same isotropic hardening rule as in the modified Cam Clay model:

$$\frac{dp'_c}{p'_c} = \frac{1 + e_0}{\lambda - \kappa} d\varepsilon_v^p \quad (3)$$

where ε_v^p = volumetric plastic strain; e_0 = initial void ratio; λ = slope of the isotropic normal compression line; and κ = slope of the swelling line.

The kinematic yield surface evolves according to a combination of isotropic and kinematic hardening rules, as follows:

$$\begin{aligned} dp'_a &= \frac{dp'_c}{p'_c} p'_a + S \left[\frac{p' - p'_a}{R} - \left(p' - \frac{p'_c}{2} \right) \right] - \frac{R^2 p'^2_c}{4} \\ ds_a &= \frac{dp'_c}{p'_c} s_a + S \left[\frac{s - s_a}{R} - s \right] \end{aligned} \quad (4)$$

where the scalar quantity S is obtained by the consistency condition for the kinematic yield surface.

The plastic flow rule is assumed to be associated and thus the plastic strain is given by:

$$d\varepsilon^p = \frac{1}{A_0 + A_1} \left\{ \frac{\partial F_y}{\partial \sigma} \right\}^T \{d\sigma\} \left\{ \frac{\partial F_y}{\partial \sigma} \right\} \quad (5)$$

where ε^p = plastic strain tensor; A_0 = hardening modulus given by the modified Cam Clay model; and A_1 = hardening modulus given by an interpolation rule. Al-Tabbaa (1987) specifies that the interpolation rule is not unique. Based on the works of Hashiguchi (1985), Al-Tabbaa (1987) proposed a hardening modulus A_1 depending on the measure of the distance between the kinematic yield surface and the bounding surface. Therefore when the two surfaces are in contact, the value A_1 is equal to 0 and only the hardening modulus A_0 is mobilized. In this study, the hardening modulus A_1 is given by:

$$A_1 = \frac{4(1 + e_0)}{\lambda - \kappa} \psi \left(\frac{b}{b_{\max} - b} \right)^\xi \left(\frac{p'_c}{2} \right)^3 R^2 \quad (6)$$

where e_0 = void ratio; ψ = material constant with ψ_c under triaxial compression and ψ_e under triaxial extension ($R_\psi = \psi_e/\psi_c$); ξ = material constant; and b_{\max} = maximal value of b equal to:

$$b_{\max} = 2p'_c(1 - R) \quad (7)$$

According to Al-Tabbaa (1987), b is the scalar product of the outward normal \mathbf{n} to the kinematic surface at the current stress state and the vector $\boldsymbol{\beta}$ which links the current stress state (point A in Fig. 1) to the stress state on the bounding surface with the same outward normal (point A' in Fig. 1).

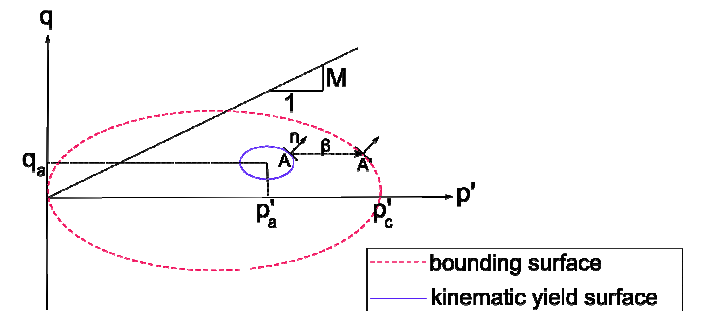


Figure 1. Representation of bounding and kinematic yield surfaces in (p', q) plan.

Model parameters can be separated into two categories: the parameters related to the monotonic be-

havior ($\nu, \kappa, \lambda, e_0, M, p'_{c0}$) and those related to the cyclic behavior (R, ψ_c, R_ψ, ξ).

We note that, in this paper, the slope of the critical state line is expressed as (Sheng et al. 2000):

$$M = M_c \left(\frac{2c^4}{1 + c^4 + (1 - c^4) \sin 3\theta} \right)^{1/4} \quad (8)$$

where θ is the Lode's angle ($\theta = -\pi/6$ under triaxial compression); M_c represents the slope of the critical state line under triaxial compression; and c is defined as follows according to Mohr-Coulomb:

$$c = \frac{3 - \sin \phi_c}{3 + \sin \phi_c} \quad (9)$$

where ϕ_c = friction angle at critical state under triaxial compression.

To introduce the anisotropy of the hardening modulus, we made the material constant ψ function of Lode's angle. Similar to M , ψ is expressed as:

$$\psi = \psi_c \left(\frac{2R_\psi^4}{1 + R_\psi^4 + (1 - R_\psi^4) \sin 3\theta} \right)^{1/4} \quad (10)$$

Therefore, R_ψ can be used to control the magnitude of plastic strains under loading and unloading conditions.

3 PARAMETER IDENTIFICATION

3.1 Principle and choice of the identification method

Inverse analysis consists in determining the set of parameters, which minimizes the difference between experimental and numerical data. In this study, the difference between experimental and numerical data, called the error function F_{err} , corresponds to the surface between the experimental and the numerical curves, i.e. the integral of the absolute value of the error (in permanent strain) during the test. Therefore, some possible isolated measurement points do not have an influence as important as by the method of square root. Inverse analysis is generally a mathematical ill-posed problem, for which the existence and uniqueness of solution are not guaranteed.

Traditionally, inverse analysis for geotechnical problems is carried out with gradient methods (Dano et al. 2006). However other optimization algorithms have been applied to geotechnical problems, as simplex method (Gioda 1985), neural network technique (Obrzud et al. 2009) or genetic algorithms (Levasseur et al. 2008). Genetic algorithms work simultaneously with a group of parameter sets. This special strategy gives to genetic methods two main advantages over other methods. Firstly, they determine a set of 'satisfactory' solutions rather than the exact mathematical one and they propose, therefore, an al-

ternative to the non-uniqueness of the solution. Secondly, by means of some modifications, genetic algorithms for mono-objective problems can be adapted for multi-objective problems. In terms of inverse analysis, a multi-objective problem makes possible the use of several experimental curves simultaneously. Because of these two interesting aspects, genetic algorithms are selected in this study.

3.2 Genetic algorithms in case of mono-objective problem

Genetic algorithms, originally introduced by Holland (1975), are derived from Darwin's evolution theory. Their principles were set and developed by Goldberg (1989). They belong to the family of stochastic algorithms and reproduce the biological process: the probability of survival of the best adapted individuals, represented here by the best set of parameters, and the probability of the multiplication of competitive ones are improved by the transmission of a favorable gene pool.

Genetic algorithms work from an initial population, i.e. a set of individuals, randomly generated among the search space. This population is modified according to a process based on the value of the error function through the following operations: selection, cross-over and mutation. Selection and cross-over improve mainly the performance of individuals, whereas mutation makes possible to continue the exploration of a given search domain and to avoid to converge prematurely towards a secondary minimum. Generation after generation, i.e. iteration after iteration, the performance of the overall population is improved. Finally the solution corresponds to an entire population of individuals with different gene pools and the result gives a global view of this set of gene pools. Contrary to deterministic algorithms, the aim of genetic algorithms is to detect individuals with low error functions, using a reduced number of iterations compared to a systematic search, rather than to guarantee the detection of an optimal set of parameters.

3.3 Multi-objective problem

A multi-objective formulation can be useful in two cases. The user wants to enrich the experimental data so that the parameter identification is more reliable. To do so, inverse analysis for several curves has to be simultaneously performed. Another reason of using multi-objective formulation is connected to the validation of constitutive model. A model can be considered as validated, if, from parameter identification using a given set of experiments, the model can reproduce other independent experiments. Therefore, if it cannot be found parameters which reproduce two or more different experiments, then the model is not relevant and cannot be validated.

Mertens et al. (2006) used multi-objective formulation for two reasons: Parameter identification and model verification. In this study, multi-objective formulation is adopted to give some information about the relevance of the model and about the trade-off, which has to be done for identification.

To solve a multi-objective problem, different resolution methods have been developed. Deb (2001) distinguishes the methods which need to make preferences before the optimization (*a priori* methods) and the ones which need to make preferences after the optimization (*a posteriori* methods). For geotechnical problems it seems difficult to decide *a priori* which test is the most reliable and especially to set the weight applied to each test. *A posteriori* methods aim at determining a so-called Pareto frontier.

If we consider five sets of parameters and the corresponding values of the error functions in case of a two-objective problem, as shown by Figure 2, we can say that the set of parameters $x^{(1)}$ fits better the first experimental curve than the set of parameters $x^{(2)}$, whereas the set of parameters $x^{(2)}$ fits better the second experimental curve than the set of parameters $x^{(1)}$. Without *a priori* preferences, we cannot say that $x^{(1)}$ is better than $x^{(2)}$ and vice versa. Originally introduced by Pareto (1897), Pareto dominance is used in order to overcome this problem. By definition, a solution $x^{(i)}$ dominates a solution $x^{(j)}$ in terms of Pareto, if both conditions of Equation 11 are fulfilled.

$$\begin{aligned} \forall m \in [1; M], F_{err}^m(x^{(i)}) &\leq F_{err}^m(x^{(j)}) \\ \exists m \in [1; M], F_{err}^m(x^{(i)}) &< F_{err}^m(x^{(j)}) \end{aligned} \quad (11)$$

where M = the number of objectives.

Considering Figure 2, $x^{(1)}$ dominates $x^{(4)}$ and $x^{(2)}$ dominates $x^{(3)}$, $x^{(4)}$ and $x^{(5)}$. $x^{(3)}$ and $x^{(5)}$ are not comparable in terms of Pareto. The solutions of a multi-objective problem correspond to the Pareto optimal solutions, which are not dominated by any others sets of parameters. In the example of Figure 2, $x^{(1)}$ and $x^{(2)}$ are equivalent solutions of the two-objective problems and $F_{err}(x^{(1)})$ and $F_{err}(x^{(2)})$ belong to the Pareto frontier. When the Pareto frontier is determined, the user can select the best set of parameters considering the Pareto frontier and others criteria related to the specific application.

Mertens et al. (2006) used the scalarization technique, which consists in building a global error function from the initial error functions, which are weighed. To determine the Pareto frontier, mono-objective optimizations are carried out with different weights. However this method cannot detect non convex parts of the Pareto frontier. Moreover a continuous variation of the weights does not imply necessarily a continuous variation along the Pareto frontier. For these reasons, the authors propose to deal with a multi-objective resolution technique and select the Multi-Objective Genetic Algorithm called MOGA because of its simplicity and its close rela-

tionship with genetic algorithms in case of classical mono-objective algorithms. MOGA has been introduced by Fonseca et al (1993). They modified the operation of selection in a classical mono-objective genetic algorithm in order to deal with a multi-objective problem. A new method of selection based on the dominance in terms of Pareto is performed. In MOGA, the performance of an individual decreases with the number of times for which the individual is dominated by another individual.

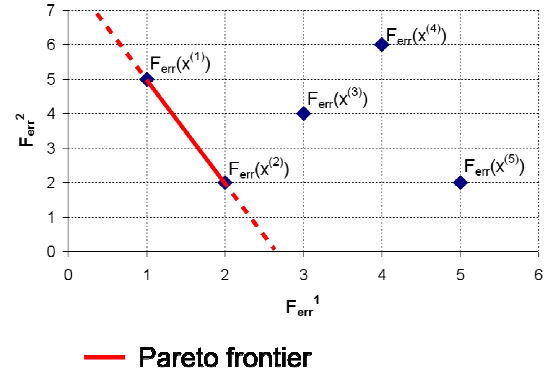


Figure 2. Solutions of a two-objective optimization.

4 APPLICATION

4.1 Undrained triaxial tests

The study considers two undrained triaxial tests on normally consolidated clay under one-way loading performed by Hicher (1979). Soil parameters directly determined from monotonic tests are summarized in Table 1. The ratio R can be determined from an isotropic compression test with unloading stage. In this study we assume $R = 0.1$, a typical value for R .

Table 1. Soil parameters for kaolinite clay.

v	κ	λ	e_0	M_c	p'_{c0} kPa
0.3	0.08	0.23	1.15	1.0	200

In this study, inverse analysis is used to determine the parameters which can not be deduced directly from experimental tests. Therefore the inverse analysis is performed on three parameters: ψ_c , R_ψ and ξ . To do so, the curve which gives the evolution of the permanent axial strain as function of the number of cycles is considered. Permanent strains are defined as the remaining strains after a cycle. Two loading levels are considered $q = 65$ kPa and $q = 84$ kPa. The maximal deviator stress obtained during an undrained triaxial monotonic test is equal to 124 kPa. Since a multi-objective problem is formulated, both error functions are divided by the number of cycles of the test, so that the error functions correspond to the mean error per cycle.

4.2 Computational program

The identification is carried out by using two different codes: the constitutive model is implemented in a FORTRAN routine and the optimization process is run by ModeFrontier, developed by ESTECO, (ModeFrontier 4). For all the optimizations the same domain is explored (Table 2).

Table 2. Studied domain.

Parameters	ψ_c	ξ	R_ψ
Minimal value	10^3	1	0.1
Maximal value	10^{16}	8	10

The initial populations contain 200 individuals. They are generated with the deterministic algorithm Sobol which is used to fill uniformly the studied domain (Sobol 1967, ModeFrontier 4). Calculations are performed during 15 generations.

4.3 Results

4.3.1 Case of mono-objective problem

Since genetic algorithms provide a set of solutions, only a limited set of the best solutions for $q = 65 \text{ kPa}$ is taken into account and summarized in Table 3. We can notice that the parameters ψ_c and ξ are closely related, whereas R_ψ seems to be independent. Small values of the parameter R_ψ are more satisfactory.

Table 3. “Satisfactory” individuals obtained with genetic method for the test $q = 65 \text{ kPa}$.

ψ_c	ξ	R_ψ	$F_{\text{err}} (\%)$
1.0e5	4	0.159	0.034
1.0e9	8	0.1	0.055
3.2e6	5	0.1	0.055
1.0e9	8	0.159	0.056
1.0e9	8	0.251	0.057
1.0e9	8	0.398	0.057

The set of parameters, which provides the best fitting between the experimental and numerical curves for $q = 65 \text{ kPa}$, is selected and the corresponding curves for both tests are plotted in Figure 3. The fitting for $q = 65 \text{ kPa}$ is satisfactory, whereas the shapes of the experimental and numerical curves for $q = 84 \text{ kPa}$ are totally different. A question remains open: Is the model or the parameter identification unsuitable?

In the same way as for the test $q = 65 \text{ kPa}$, Table 4 showed a limited set of the best solutions for $q = 84 \text{ kPa}$. The same comments as for $q = 65 \text{ kPa}$ can be done except that higher values of R_ψ seem slightly more satisfactory.

Figure 4 represents the experimental and numerical curves for the best set of parameters. The fitting for both tests is better than for the previous inverse analysis. However the shape of the numerical curve for both tests is not well captured. The (quasi-) stabi-

lization occurring during both tests does not appear contrary to the previous inverse analysis.

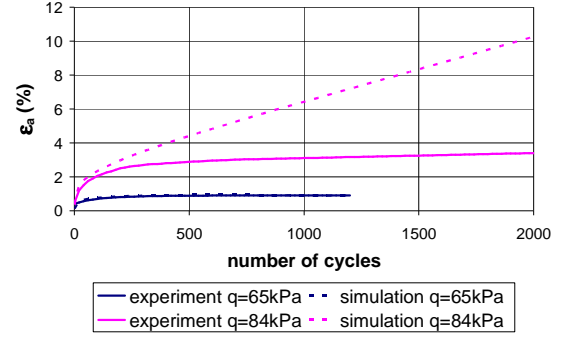


Figure 3. Comparison of the experimental and numerical cyclic curves for the best set of parameters for $q = 65 \text{ kPa}$.

Table 4. “Satisfactory” individuals obtained with genetic method for the test $q = 84 \text{ kPa}$.

ψ_c	ξ	R_ψ	$F_{\text{err}} (\%)$
1e9	8	2.512	0.2177
1e9	8	3.981	0.2177
1e9	8	1.585	0.2177
1e9	8	1	0.2180
1e9	8	0.631	0.2181
1e9	8	0.398	0.2185

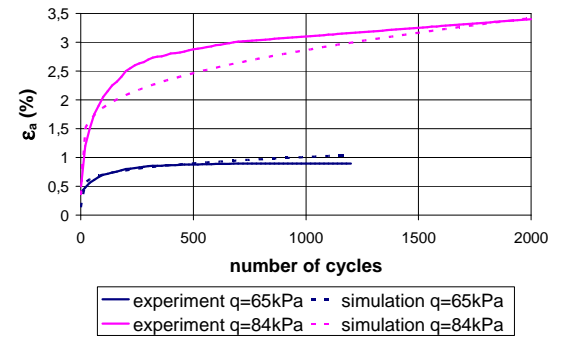


Figure 4. Comparison of the experimental and numerical cyclic curves for the best set of parameters for $q = 84 \text{ kPa}$.

4.3.2 Case of multi-objective problem

The question remained open in the previous section can be answered thanks to a multi-objective formulation. If no satisfactory tradeoff can be determined by the multi-objective problem, then the relevance of model can be discussed. Otherwise, the uncertainty of the identification can be removed. Figure 5 shows the solutions of the multi-objective problem in the criterion space. The non-dominated solutions are encircled and are summarized in Table 5. The best sets of parameters obtained with both mono-objective inverse analyses can be found again (I1 and I9) and the comments about the sensitivity of R_ψ can also be noticed.

The difference between the numerical curves of the sets of parameters from I2 to I9 is so small that I9 can be used as reference and the best set of parameters obtained with the mono-objective inverse analysis for $q = 84 \text{ kPa}$ can be considered as a good tradeoff between both experiments.

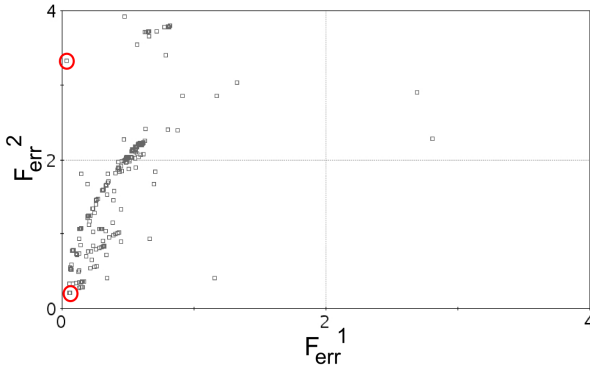


Figure 5. Distribution of solutions of the multi-objective optimization in the criterion space.

Table 5. Non-dominated solutions obtained with multi-objective genetic method.

	ψ_c	ξ	R_ψ	F_{err}^1 (%)	F_{err}^2 (%)
I1	1.0e5	4	0.159	0.0339	3.3312
I2	1.0e9	8	0.1	0.0550	0.2196
I3	1.0e9	8	0.159	0.0564	0.2193
I4	1.0e9	8	0.251	0.0573	0.2186
I5	1.0e9	8	0.398	0.0577	0.2185
I6	1.0e9	8	0.631	0.0582	0.2181
I7	1.0e9	8	1.000	0.0582	0.2180
I8	1.0e9	8	1.585	0.0583	0.2177
I9	1.0e9	8	2.512	0.0584	0.2177

5 CONCLUSIONS

A modification was made on the two-surface model of Al-Tabbaa (1987) to describe undrained cyclic behavior of clay with high number of cycles. A method of soil parameter identification accounting for the characteristics of inverse analysis was proposed.

The method of parameter identification shows the multiple assets of genetic algorithms. Contrary to traditional algorithms, genetic algorithms provide a set of solutions, which seem to be consistent with the non-uniqueness of the solution of inverse analysis. The analysis of this set of solutions gives information about the sensitivity of the model parameters and their coupling effects. The formulation of problem as multi-objective makes possible the use of several tests simultaneously. As a result, model parameters can be more efficiently identified. If no tradeoff concerning the model parameters can be determined from different tests, then the relevance of the model can be discussed.

The proposed method of identification was applied to identify model parameters from two undrained triaxial tests on clay under one-way loadings. Satisfactory identification of a tradeoff from both tests was obtained. However the (quasi-) stabilization of permanent strain observed during the experiments cannot be very well captured. The perspectives of the study concern the application of the new method to tests on natural clays.

REFERENCES

- Al-Tabbaa, A. 1987. Permeability and stress-strain response of speswhite kaolin. PhD thesis, University of Cambridge, Cambridge, UK.
- Andersen, K.H. 2009. Bearing capacity under cyclic loading offshore, along the coast, and on land. *Can. Geotech. J.* 46:513-535.
- Dafalias, Y.F. & Hermann, L.R. 1982. Bounding surface formulation of soil plasticity. In G.N. Pande & O.C. Zienkiewicz (eds), *Soil Mechanics – Transient and Cyclic Loads*: 253-282. Chichester: John Wiley & Sons.
- Dano, C., Hicher, P.-Y., Rangeard D. & Marchina P. 2006. Interpretation of dilatometer tests in a heavy oil reservoir. *Int. J. Numer. Anal. Methods Geomech.* 31:1197-1215.
- Deb, K. 2001. Multi-Objective Optimization using Evolutionary Algorithms. Chichester: John Wiley & Sons.
- Fonseca, C.M. & Fleming, P.J. 1993. Genetic algorithms for multi-objective optimization: Formulation, discussion and generalization. In S. Forrest (ed), *Genetic algorithms: Proceedings of the Fifth International Conference, Urbana-Champaign, IL, USA, 7-22 July 1993*. San Mateo: Morgan Kaufmann Publishers Inc.
- Gioda, G. Some remarks on back analysis and characterization problems in geomechanics. . In T. Kawamoto & Y. Ichikawa (eds), *Proceedings of the 5th International Conference on Numerical Methods in Geomechanics, Nagoya, 1-5 April 1985*. Rotterdam: Balkema.
- Goldberg, D.E. 1989. Genetic algorithms in search, optimization and machine learning. Reading, MA: Addison-Wesley.
- Hashiguchi, K. 1985. Two- and three-surface models of plasticity. In T. Kawamoto & Y. Ichikawa (eds), *Proceedings of the 5th International Conference on Numerical Methods in Geomechanics, Nagoya, 1-5 April 1985*. Rotterdam: Balkema.
- Hicher, P.-Y. 1979. Contribution à l'étude de la fatigue des argiles. PhD Thesis, Ecole Centrale des Arts et Manufactures, Paris, France.
- Holland, J.H. 1975. Adaptation in Natural and Artificial Systems. Ann Arbor, MI: University of Michigan Press.
- Levasseur, S., Malécot, Y., Boulon, M. & Flavigny, E. 2008. Soil parameter identification using a genetic algorithm. *Int. J. Numer. Anal. Methods Geomech* 32:189-213.
- Mertens, J., Stenger, R. & Barkle, G.F. 2006. Multiobjective Inverse Modeling for Soil Parameter Estimation and Model Verification. *Vadose Zone J.* 5:917-933.
- ModeFrontier 4, User Manual, Esteco, Trieste, Italy.
- Mroz, Z. 1967. On the description of anisotropic hardening. *J. Mech. Phys. Solids*, 15:163-175.
- Muir Wood, D. 1991. Approaches to modelling the cyclic stress-strain response of soils. In M.P. O'Reilly & S.F. Brown (eds), *Cyclic loading of soils: From theory to design*: 18-69. London: Blackie and Son.
- Obrzud, R.F., Vulliet, L. & Truty, A. 2009. A combined neural network / gradient-based approach for the estimation of constitutive model parameters using self-boring pressuremeter tests. *Int. J. Numer. Anal. Methods Geomech.* 33:817-849.
- Pareto, V. 1897. Cours d'Economie Politique. Lausanne, Rouge.
- Sheng, D., Sloan, S.W. & Yu, H.S. 2000. Aspects of finite element implementation of critical state models. *Comput. Mech.* 26:185-196.
- Sobol, I.M. 1967. Distribution of points in a cube and approximate evaluation of integrals. *U.S.S.R Comput. Maths. Math. Phys.* 7: 86-112.